Research Article

Journal of PeptideScience

Received: 11 April 2011 Revised: 3 June 2011 Accepted: 10 June 2011 Published online in Wiley Online Library: 18 July 2011

(wileyonlinelibrary.com) DOI 10.1002/psc.1393

Effect of charge, topology and orientation of the electric field on the interaction of peptides with the α-hemolysin pore

Christopher Christensen, Christian Baran, Besnik Krasniqi, Radu I. Stefureac, Sergiy Nokhrin and Jeremy S. Lee*

Nanopore analysis is an emerging technique of structural biology which employs nanopores, such as the α-hemolysin pore, as a biosensor. A voltage applied across a membrane containing a nanopore generates a current, which is partially blocked when a molecule interacts with the pore. The magnitude (*I*) and the duration (*T*) of the current blockade provide an event signature for that molecule. Two peptides, CY12(+)T1 and CY12(−)T1 with net charges +2 and −2, respectively, were analysed using different applied voltages and all four possible orientations of the electrodes and pore. The four orientations were vestibule downstream (VD), vestibule upstream (VU), stem downstream (SD) and stem upstream (SU) where vestibule and stem refer to the side of the pore on which the peptide was placed and downstream and upstream refer to the application of a positive or negative electrophoretic force, respectively. For CY12(+)T1, the effect of voltage on the event duration was consistent with translocation in the VD and SD configurations, but only intercalation events were observed in the VU and SU configurations. For CY12(−)T1, translocations were only observed in the VD and VU configurations. The results are interpreted in terms of two energy barriers on either side of the lumen of the pore. The difference in height of the barriers determines the preferred direction of exit. Electroosmotic flow and current rectification due to the pore as well as the dipole moment and charge of the peptide also play significant roles. Thus, factors other than simple electrophoresis are important for determining the interaction of small peptides with the pore.

Keywords: α-hemolysin; peptide; translocation; intercalation; electrophoresis; electroosmosis; rectification

Introduction

Some bacterial toxins, such as α-hemolysin of *Staphylococcus aureus*, have the ability to form pores which puncture eukaryotic cell membranes and cause an increase in permeability to ions and small molecules [1,2]. Experimentally, the pores can be exploited to study the properties of single molecules; so called nanopore analysis [3–9]. Briefly, the pore will self-assemble into a lipid membrane seperating two chambers such that the vestibule of the pore is facing the chamber to which the toxin was applied; i.e. the *cis* side. When a voltage is applied across the pore a constant current will be recorded. For example, in a buffer of 1 M KCl at neutral pH, a voltage of 100 mV induces a current of 100 pA. If a single polynucleotide, peptide or protein interacts with the pore there will be a decrease in the current, *I*, for a time, *T* which can be measured by standard patch clamp techniques. Recently, nanopore analysis has generated considerable interest in biotechnology and medical diagnostics because of the possibility of relating the parameters *I* and *T* to the sequence and/or structure of individual molecules.

Originally, nanopore analysis using α-hemolysin was applied to polynucleotides with the long-term goal of rapid sequencing of single DNA molecules [10–14]. In general, two types of events can be envisaged; bumping events, in which the DNA briefly interacts with the pore before diffusing away and translocation events in which the molecule threads through the pore and exits on the *trans* side [15]. DNA has a high negative charge density and there is good evidence that it is electrophoretically driven through the pore towards the positive electrode. For example, the DNA can be collected from the *trans* chamber and amplified by PCR [15]. More recently, nanopore analysis has been applied to peptides and proteins. For example, collagen-like, β-turn, α-helical, hydrophobic and Zn-finger peptides as well as histidine containing protein, myelin basic protein, maltose-binding protein and prion proteins have all been studied with the α-hemolysin pore [16–30]. Similar bacterial pores such as aerolysin and OmpF as well as solid state pores have also proved useful [19,23,31–34]. It is clear that size, overall charge, hydrophobicity, degree of folding and dipole moment all affect the event parameters in a somewhat predictable manner. However, in some cases the peptide or proteins were uncharged or carried a net positive charge, so they cannot be driven through the α-hemolysin pore with the electric field [21,30]. Therefore, the evidence for translocation of peptides or proteins is indirect at best. For the case of a neutral molecule, β-cyclodextrin, it was shown that electroosmosis was also important for translocation through the α-hemolysin pore [35]. Similarly, work with solid state pores has also revealed some 'anomalous' behavior (i.e. non-electrophoretic) and it was demonstrated that electroosmotic effects can predominate for the translocation of some proteins at low pH [26].

* *Correspondence to: Jeremy S. Lee, Department of Biochemistry, 107 Wiggins Road, University of Saskatchewan, SK, Canada S7N 5E5.*
E-mail: jeremy.lee@usask.ca

Department of Biochemistry, 107 Wiggins Road, University of Saskatchewan, SK S7N 5E5, Canada

Journal of PeptideScience

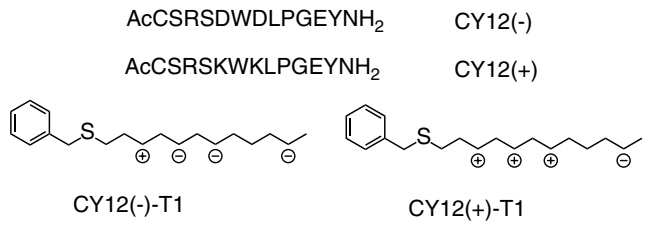

Figure 1. Sequence of linear CY12(−) and CY12(+) and the structure of CY12(−)T1 and CY12(+)T1. CY12(−) has a net charge of −2 and CY12(+) has a net charge of +2. Each node represents a single amino acid residue. Charged residues are indicated with a + or −.

Recently, a third type of event, called intercalation, was identified for the interaction of tethered peptides with the α-hemolysin pore [36]. Briefly, intercalation occurs when the peptide enters the lumen of the pore from one side and exits from the same side without translocating. Intercalation has also been observed by attaching the peptide to a protein. The peptide can enter the pore but is prevented from translocating by the much larger protein [37]. For a translocation event with a favourable electric field (i.e. electrophoretically driven), the time is expected to decrease as the voltage increases. For an intercalation event in the same orientation, the time increases as the voltage is increased because, once inside the pore, the peptide must diffuse back against the electric field. Thus, translocation and intercalation events are expected to have similar blockade currents but the effect of voltage will be opposite.

In this article, we have studied the effect of charge, topology and orientation of the electric field on the interaction of dodecamer peptides with the α-hemolysin pore in order to understand what factors allow translocation to occur. The sequence of the peptides CY12(+) and CY12(−) is shown in Figure 1. A toluene group was attached *via* the thiol of the terminal cysteine to yield CY12(+)T1 and CY12(−)T1 as it has been shown that the presence of a hydrophobic terminal residue increases the ratio of translocation to bumping events [19,36]. The event parameters were measured at different voltages and for the four possible orientations of the electrodes and the pore (Figure 2) as it was anticipated that translocation from vestibule to stem would be different than from stem to vestibule. For simplicity, these orientations have been called vestibule upstream (VU), vestibule downstream (VD), stem upstream (SU) and stem downstream (SD), where upstream denotes against, and downstream denotes with the electric field. Note that 'upstream' and 'downstream' are opposite for peptides of opposite charge. Our results show that factors other than electrophoresis determine whether a peptide intercalates or translocates.

Materials and Methods

Synthesis of Peptides

CY12(+) and CY12(−) (American Peptide Company Inc., Sunnyvale, CA, USA) were linked to toluene by the reaction of the terminal cysteine with bromotoluene [28]. CY12(+)T1 and CY12(−)T1 were purified by HPLC and the identity was confirmed by MALDI-TOF mass spectrometry (expected and calculated masses within 0.1%) [38].

Preparation of Membrane

An aliquot of 1,2-diphytanoyl-*sn*-glycero-3-phosphocholine (Avanti Polar Lipids Inc., Alabaster, AL, USA) dissolved in $CHCl_3$ was dried under a vacuum for 4 h to evaporate the solvent. This aliquot was then dissolved in 25 µl of decane to produce a solution of a final concentration of 30 mg/ml and left to incubate for 30 min at 22 ± 2 °C. A layer of this solution was painted on to the aperture on each side of the perfusion cup (Warner Instruments, Hamden, CT, USA) using a paintbrush and then dried under a stream of nitrogen and then a second layer was applied to each side and dried. At this point, the perfusion cup was placed on an active-air-floating-table (Kinetic Systems, Boston, MA, USA) inside of a Faraday cage (Warner Instruments). One millilitre of 1 M KCl, 10 mM phosphate buffer (pH 7.8) was added to both the *cis* and *trans* sides of the perfusion cup. The membrane was thinned to a bilayer through repeated brush strokes and use of a syringe. A bilayer was achieved when the membrane reached a capacitance of about 70 pF as measured by Ag/AgCl electrodes attached to a BC-535 headstage connected to a BC-535 amplifier (Warner Instruments).

Insertion of Pore and Addition of Peptide

Initially, 7.5 µl of 1.6 µg/ml α-HL (Sigma Aldrich) in 1 M KCl, 10 mM phosphate buffer (pH 7.8) was added to the perfusion cup near the aperture on the side where the pore was to be inserted. If a pore failed to insert within 2 min, another 5 µl was added at 2-min intervals until a stable pore was achieved. A pore was deemed to be acceptable for recording if the measured current was +100 ± 2 pA per pore at +100 mV (*cis* to *trans*). The electrodes were reversed if the experiment required it at this stage. Twenty microlitre of a 1.0 mg/ml solution of CY12(+)T1, or 5–20 µl of a

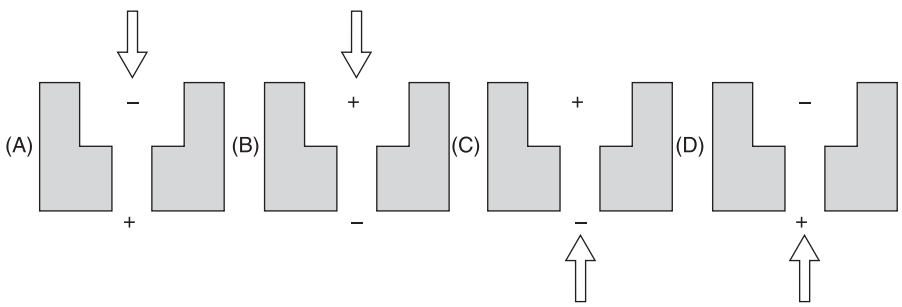

Figure 2. Cartoon of possible configurations for α-HL pore and electrodes for a positively charged molecule. (A) VU, (B) VD, (C) SU, (D) SD. The top of the cartoon is the vestibule and the bottom the stem. The charge represents the charge of the electrodes and the arrow represents the point of entry of the peptide. For a negatively charged molecule, (A) and (C) are downstream configurations and (B) and (D) are upstream configurations.

2.0 mg/ml solution of CY12(−)T1 was added to the electrolyte on the appropriate face of the perfusion cup near the aperture.

Recording of Events

Data was recorded at a temperature of 22 ± 2 °C. The signal recorded by the Ag/AgCl electrodes attached to the BC-535 headstage (Warner Instruments,) was passed through a BC-535 amplifier under voltage clamp conditions and sampled at 100 kHz. The signal was then filtered through an LPF-8 low pass 8 pole Bessel filter (Warner Instruments) at 10 kHz. This signal was passed through an Axon Instruments Digidata 1440A (Axon Instruments, Union City, CA, USA) digitizer and recorded on a Windows XP 64-bit workstation running Clampex 10.1 (Axon Instruments). The recorded data was analysed using Clampfit 10.1 (Axon Instruments) using two threshold levels which detected events with current blockades of −10 and −50 pA. As the rise time of the 10 kHz filter used was 0.033 ms and an accurate measurement is possible only for events with durations twice the rise time value, all events with blockade durations faster than 0.066 ms were discarded [39,40]. (It should be noted that after fitting to an exponential, the characteristic time can be less than this value). The durations and amplitudes of all events were imported in Origin 7.0 (OriginLab Corporation, Northamton, MA, USA) and ploted as histograms against the number of events. The bin sizes used were 1 pA and 0.05 ms for the blockade current and duration, respectively. The current blockade histograms were fit with the Gaussian function and blockade time histograms were fit with a single exponential function as described previously [19,22,23]. Curve fitting was done using the Levenberg–Marquardt method and the standard deviation of the function was used to evaluate the goodness of fit [39]. Each experiment was repeated at least twice. The estimated errors are ±1 pA for the blockade current and ±10% for the blockade times.

Results

Preliminary experiments showed that the measured current was smaller at positive voltages (i.e. when the positive electrode was on the vestibule side of the pore) than at the same negative voltage. As shown in Figure 3, the current/voltage curve is linear between 0 and +150 mV but some rectification is apparent between 0 and −150 mV. Thus, at −150 mV the current is only 105 pA. Current traces for CY12(+)T1 in all four configurations at 100 mV are shown in Figure 4. Each spike represents an event. For a small peptide, events with a current blockade of 20–30% (i.e. 20–30 pA at 100 mV) occur when the peptide bumps into the pore before diffusing away. Such bumping events can be seen in the VD and VU configurations (Figure 4(A) and (B)) but are very infrequent in the SD and SU configurations (Figure 4(C) and (D)). The larger spikes are due to events in which the peptide enters the pore resulting in a larger current blockade of about 70%. However, as was demonstrated recently with analogues of CY12(+)T1, it is difficult to distinguish between translocation and intercalation events without assessing the effect of voltage on event times [36].

Therefore, CY12(+)T1 was examined at 50, 100 and 150 mV and the current blockade histograms are shown in columns 1 and 3 of Figure 5. The corresponding current time histograms for the peak at about 70% current block are shown in columns 2 and 4 of Figure 5. The current time histograms for the bumping

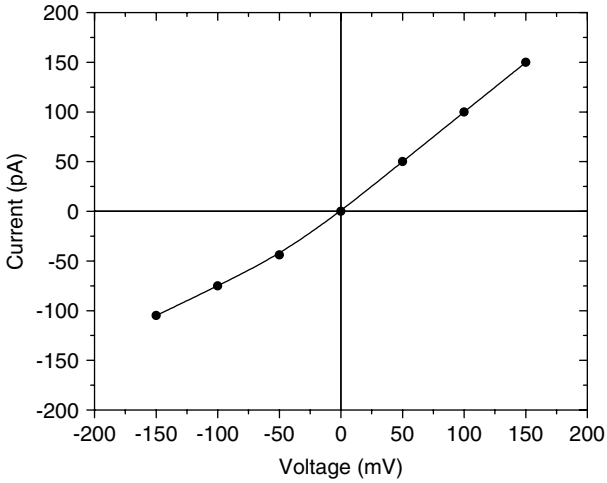

Figure 3. Current rectification with the α-hemolysin pore. Each point is the average of at least five measurements and the error is too small to be shown.

peak, if present, are not shown, but the corresponding event parameters are listed in Table 1 for both bumping events (I_1 and T_1) and for the events at about 70% current block (I_2 and T_2). For the SD (Figure 5(M)–(O)) and SU (Figure 5(S)–(U)) configurations there were an insufficient number of bumping events to allow a meaningful analysis. Except perhaps for the VD configuration (Figure 5(A)–(C)), there is a good fit to a Gaussian distribution for the current blockade peaks and a good fit to a single exponential for the blockade times. It is noticeable that the Gaussian peaks in the VU (Figure 5(G)–(I)) and SD (Figure 5(M)–(O)) configurations for which the negative electrode is on the vestibule side of the pore, are sharper (i.e. smaller width at half height) than in the VD and SU configurations. For the VU and SD configurations, the % blockade of the major peaks does not change significantly with voltage presumably, because the volume occluded by the peptide is constant. For VD and SU, there is an apparent decrease in the % block as the voltage increases which may be related to the voltage rectification described in Figure 3. In the VU configuration, the proportion of bumping events increases with voltage and a small third peak appears at 150 mV, which may represent a different conformation or orientation of the peptide but this has not been included in the analysis.

In the VD configuration, the T_2 blockade times (Table 1) decrease from 1.05 ms at 50 mV to 0.34 ms at 150 mV, which is consistent with translocation because the positively charged peptide is being electrophoretically driven to the negative electrode. In the VU configuration T_2 also decreases from 1.43 to 0.60 ms as the voltage is increased from 50 to 150 mV but the peptide is not being electrophoretically driven and so is not consistent with translocation. Similarly, the T_2 values decrease with increasing voltage in the SD configuration (1.66–0.64 ms) and in the SU configuration (0.58–0.34 ms) (Table 1). Again these voltage effects are consistent with translocation for the SD but not the SU configuration.

Current traces for CY12(−)T1 in all four configurations are shown in Figure 6. As will be discussed below the event frequencies in VD and SD were significantly greater than for VU and SU. The corresponding blockade current and blockade time histograms are shown in Figure 7 in the same format as Figure 5. Again for simplicity, the blockade time histograms for the bumping events are not shown but all the event parameters are summarised in

Journal of PeptideScience

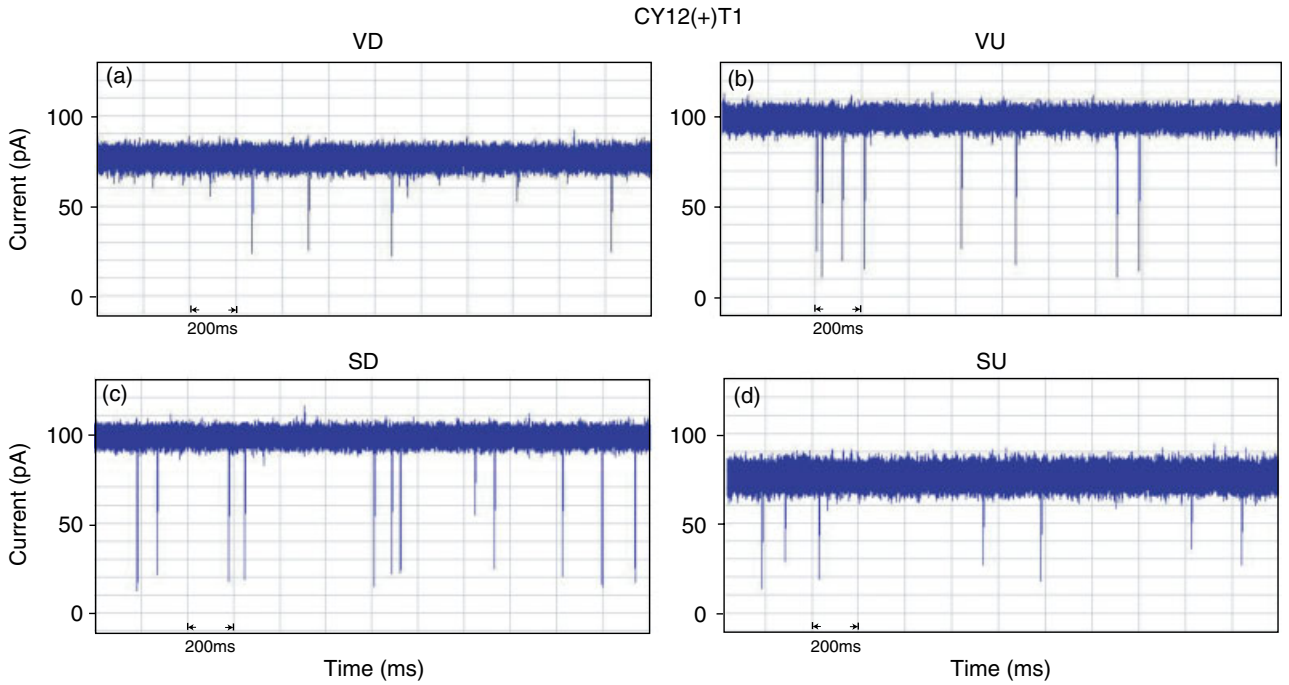

Figure 4. Traces of CY12(+)T1 in VD, VU, SD and SU configurations under 100 mV applied potential. Note the rectified open pore current (OPC) in VD and SU configurations.

Table 2. For VD (Figure 7(A)–(C)), a small third peak is present at 100 and 150 mV. As was the case with CY12(+)T1, these effects are likely due to multiple conformations or orientations of the peptide as it enters the pore. In contrast to the positively charged peptide, for CY12(−)T1 in VU (Figure 7(G)–(I)) and SD (Figure 7(M)–(O)) configurations there is a significant increase in the % blockade current as the voltage is increased. Finally, the proportion of bumping events increases significantly with increasing voltage for VD (5–32%) and for SU (6–56%) but decrease for the VU (18–2%) and SD configurations (6% to <1%).

As shown in Table 2, in all configurations the T_2 values for CY12(−)T1 are much smaller compared to those for CY12(+)T1 especially at 50 mV where the difference is an order of magnitude. For VD the T_2 values decrease (0.19–0.08 ms) with increasing voltage consistent with translocation as described previously [27]. For SU, the T_2 values also decrease (0.13–0.07 ms) but as this is an upstream configuration it is consistent with an intercalation type of event. Suprisingly, with increasing voltage the T_2 values increase for VU (0.16–0.30 ms), which is consistent with translocation upstream and increase for SD (0.06–0.31 ms), which is not consistent with translocation downstream. Thus, it would appear that CY12(−)T1 cannot translocate from the stem side of the pore but can translocate from the vestibule either downstream or upstream.

Discussion

The major goal of this work was to understand the effect of charge and orientation on the interaction of small peptides with the α-hemolysin pore. Previously, it was assumed that the behavior of small charged peptides would be dominated by electrophoresis. Thus, for a downstream configuration, frequent translocations are expected, the % blockade should be independent of voltage and the blockade time should decrease with increasing voltage [18,21,30]. From the results presented above, it is clear that factors other than electrophoresis play a role.

First, the % blockade current does change with voltage when there is current rectification. The α-hemolysin pore shows some anion selectivity due to the presence of an excess of lysine residues in the constriction on the vestibule side of the lumen [35]. Thus, when the positive electrode is on the vestibule side of the pore there is a voltage-dependent build up of Cl^- at the constriction, which reduces the effective voltage and the measured current. For example, for CY12(+)T1 in the VD configuration the % blockade decreases with increasing voltage but these are most likely translocation events because there is a concomitant reduction in event time (Table 1). Similarly, for events which are most likely to be intercalation such as CY12(+)T1 in the SU configuration the % blockade current also decreases with voltage. Therefore, a constant % blockade current cannot be used to distinguish translocation from intercalation.

Second, the event times for translocation and intercalation are nearly an order of magnitude larger in all configurations for CY12(+)T1 compared to CY12(−)T1. One possible explanation is that the positive peptide binds more tightly to the lumen of the pore than the negative peptide resulting in a longer dwell time. Alternatively, the asymmetry of the pore may be the cause because the anion selectivity will result in an electroosmotic flow towards the positive electrode [35]. The magnitude of electrophoretic and electroosmotic flow are both proportional to the applied voltage [41]. Thus, in all configurations the electrophoretic and electroosmotic flow are subtractive for the positive peptide but additive for the negative peptide. In other words, the combined force is always smaller for CY12(+)T1 compared to CY12(−)T1. The ability to slow down the rate of translocation is important for sequencing technologies since the time which each subunit of the polymer spends in the pore determines how accurately it can be

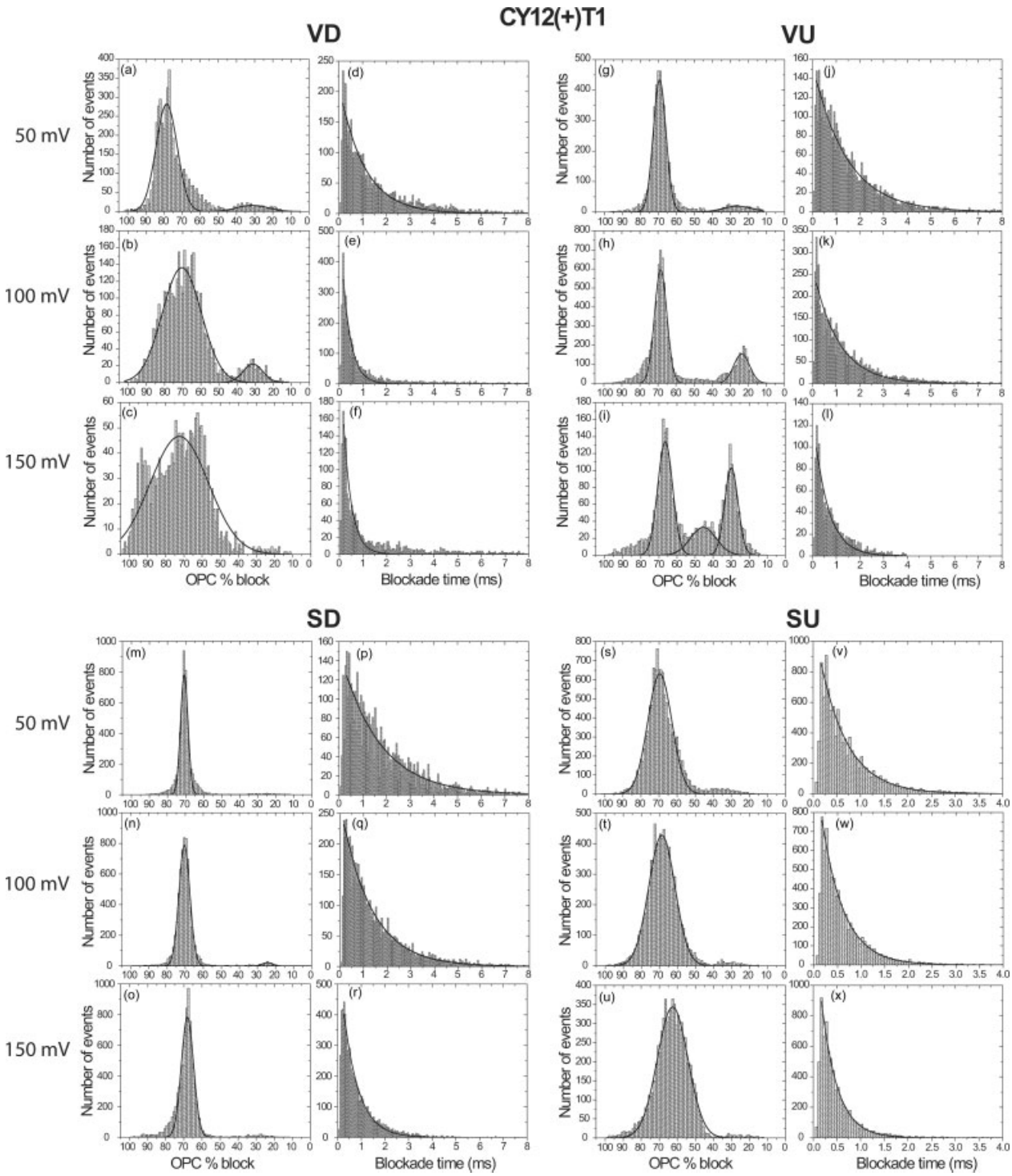

Figure 5. Histograms of the % OPC and blockade time versus the number of events for CY12(+)T1 peptide in VD, VU, SD and SU configurations under applied potentials of 50, 100 and 150 mV. The blockade time histograms for the bumping events are not shown but the *T* values are listed in Table 1.

interrogated. Clearly, this can be achieved by arranging for the two forces to oppose each other.

Third, the magnitude of the voltage has a large effect on the proportion of bumping events for CY12(−)T1 (Figure 7). Again there is clear evidence for asymmetry as the proportion increases for VD and SU (i.e. when the positive electrode is on the stem side) and decreases for VU and SD (i.e. when the positive electrode is on the vestibule side). One possibility is that there is a preferred orientation for the linear peptide when it is present in the lumen of the pore. If we assume, for the moment, that this orientation has the toluene tether pointing towards the stem side then the excess negative charge (Figures 1 and 8) of the peptide will be mostly oriented towards the vestibule side. Now, the dipole of this peptide is in the opposite direction (i.e. carboxy terminus to tether) and therefore as the peptide approaches the pore, the electric field will tend to orient the peptide so that the tether is

Journal of PeptideScience

Table 1. Event parameters for CY12(+)T1 in all four configurations

Configuration	Translocation/ intercalation peak (% block)	Bumping peak (% block)	Translocation/ intercalation time (ms)	Bumping time (ms)
50 mV				
VD	79	32	1.05	0.10
VU	69	26	1.43	0.04
SD	70	–	1.66	–
SU	70	–	0.58	–
100 mV				
VD	71	31	0.36	0.04
VU	68	24	1.07	0.14
SD	70	–	1.29	–
SU	69	–	0.46	–
150 mV				
VD	72	–	0.34	–
VU	67	30	0.60	0.09
SD	68	–	0.64	–
SU	63	–	0.34	–

The errors are estimated to be ±1% for the % blockade current and ±10% for the blockade times.

towards the negative electrode. In other words, in the VD and SU configurations the peptide will have to reorient against the electric field in order to achieve the preferred orientation in the lumen of the pore; as the voltage increases there will be more bumping events. For the VU and SD configurations, the electric field will promote the correct orientation of the peptide as it approaches the pore, so that increasing the voltage will decrease the number of bumping events. Reorientation effects may be less pronounced for CY12(+)T1 as in this case the excess of positive charge is in the middle of peptide so the dipole moment is expected to be smaller compared to CY12(−)T1.

Fourth, for CY12(+)T1 in the VD and SD configurations there is good evidence for translocation since the event time decreases with increasing voltage, as expected. Similarly, it would appear that CY12(+)T1 mostly intercalates in VU and SU since the event time also decreases with increasing voltage. However, for CY12(−)T1 this simple behavior does not occur. For CY12(−)T1 with VU, the event time increases with increasing voltage suggesting that the peptide is translocating against the electric field. For CY12(−)T1 with SD, the event time also increases with increasing voltage, which would be expected for intercalation. To explain these results, we propose that the peptide diffuses or is driven into the lumen of the pore through an energy barrier B1 from the vestibule or through B2 from the stem side (Figure 8(A)). The energy barriers are due to (i) entropic costs arising from reorientation of the peptide into a suitable conformation; (ii) repulsive (or attractive) forces from interaction of the peptide with the functional groups on the pore; (iii) and electrical forces including electrophoresis, electroosmosis and current rectification [20,41]. The resulting energy diagram is shown in Figure 8(B). Without rectification (i.e. VD and SU for CY12(−)T1), the peptide enters the pore from either direction and then binds in the lumen. As B1 is larger than B2, the peptide is more likely to exit to the stem side regardless of which side it entered. When the polarity is reversed, it might be expected that the energy difference between the two barriers would be reversed. However, as shown in Figure 3, the pore rectifies the flow of Cl^- when the positive electrode is on the vestibule side leading to a build up of negative charge. In turn, this repels the peptide so that B1 is still larger than B2. Thus, for VU and SD, CY12(−)T1 enters the pore, binds in the lumen and preferentially exits on the stem side.

If this model is correct, then we would predict that the frequency of (Translocation/Intercalation) events (Table 3) should be determined by the height of the energy barriers. Thus, for CY12(−)T1 with the positive electrode on the vestibule side, $\Delta E(B1\text{-}V) > \Delta E(B2\text{-}S)$ and indeed the frequency of VU is significantly less than SD. Similarly, when the polarity is reversed

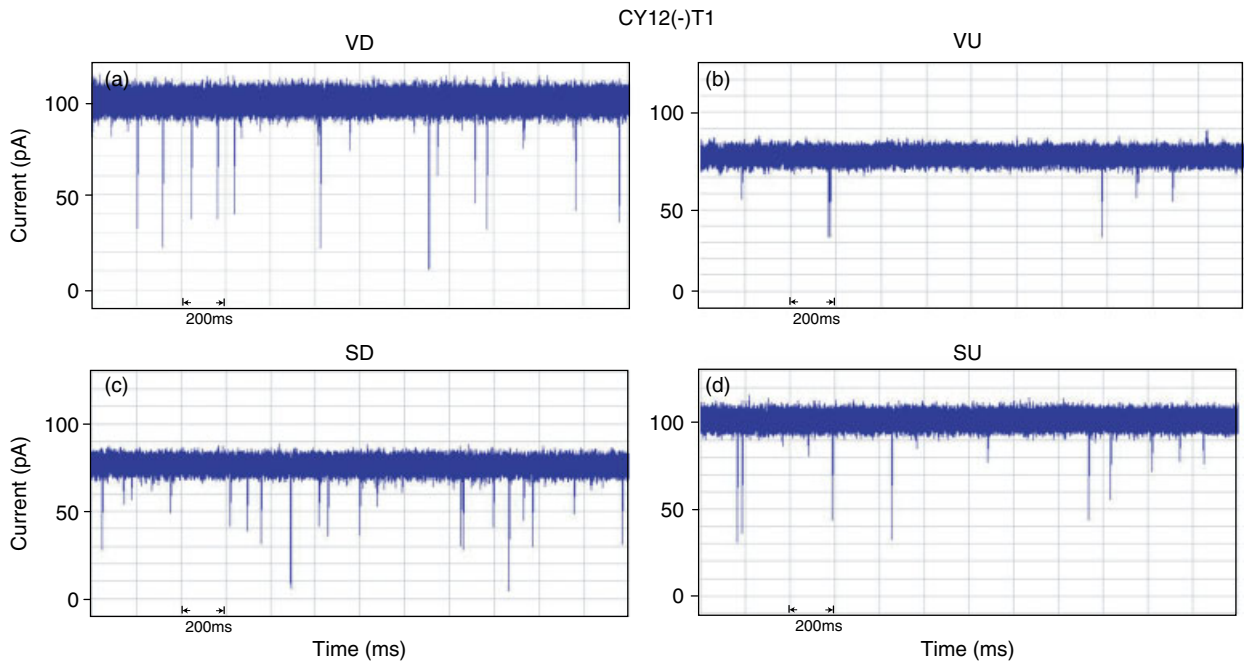

Figure 6. Traces of CY12(+)T1 in VD, VU, SD and SU configurations under 100 mV applied potential. Note the rectified OPC in VU and SD configurations.

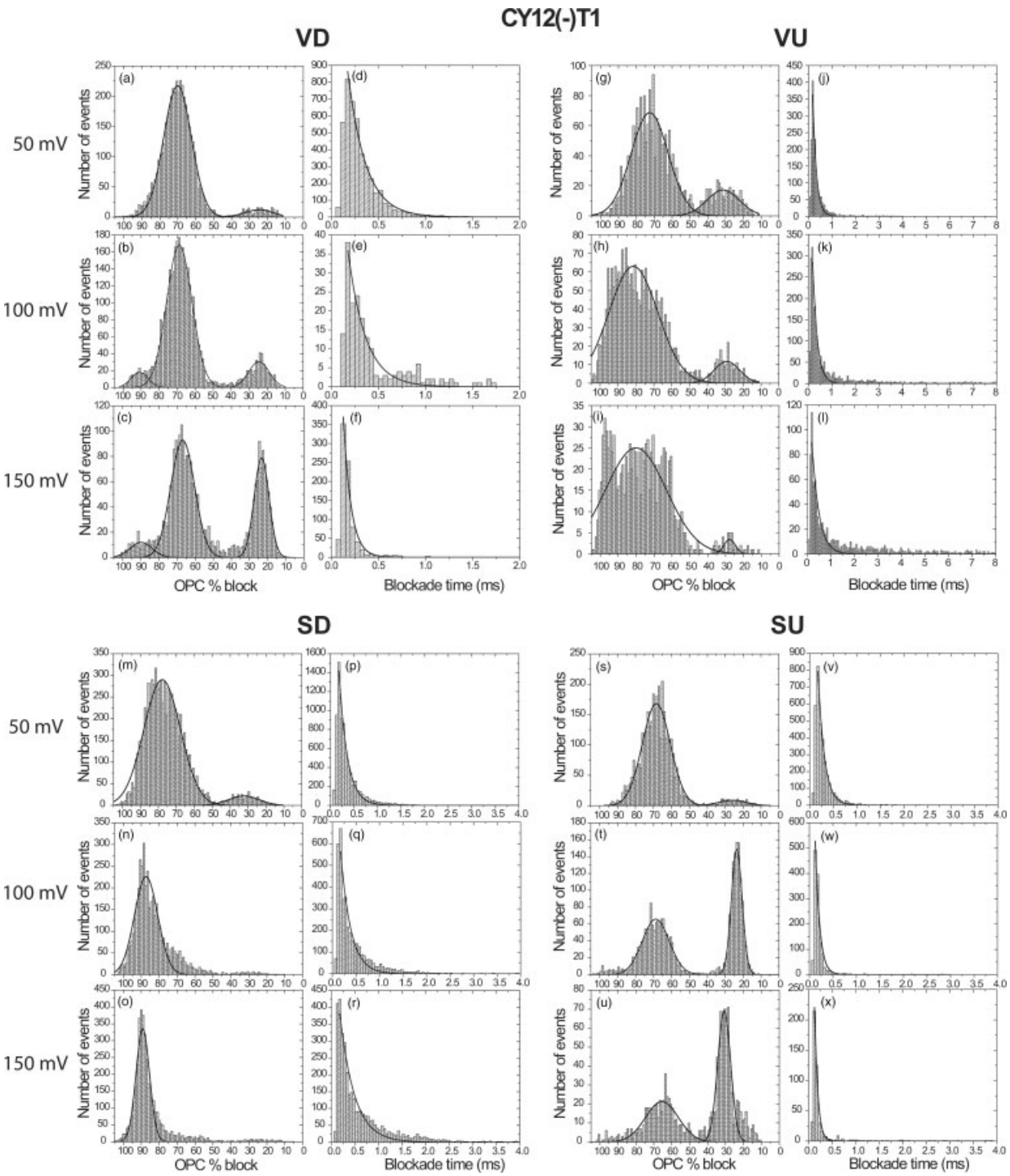

Figure 7. Histograms of the % OPC and blockade time versus the number of events for CY12(−)T1 peptide in VD, VU, SD and SU configurations under applied potentials of 50, 100 and 150 mV. The blockade time histograms for bumping events are not shown but the *T* values are listed in Table 2.

$\Delta E(B2\text{-}S) > \Delta E(B1\text{-}V)$ and the frequency of VD events is an order of magnitude greater than SU events. For CY12(+)T1, the increase in event times reveals that either the energy well in the lumen is much deeper or that both B1 and B2 are of higher energy. Therefore, the effects of rectification will be smaller and electrophoretic forces will dominate in both directions, so that smaller differences in event frequencies are observed. It should be noted that the above discussion does not imply all-or-none behavior. If B1 and B2 have similar energies, then both translocations and intercalations will occur and thus the effect of voltage on event times may be small. As the difference in event times for intercalation and translocation are small (especially for CY12(−)T1), it was not possible to resolve the time histograms into two exponentials. Thus, for any distribution it is only possible to conclude whether intercalation or translation predominates.

Finally, these results are relevant to the interaction of proteins with α-hemolysin and solid state pores. The CY12-T1 peptides have formal net charges of ± 0.17 per amino acid residue. The net

Journal of PeptideScience

Table 2. Event parameters for CY12(−)T1 in all four configurations

Configuration	Translocation/ Intercalation peak (% block)	Bumping peak (% block)	Translocation/ Intercalation time (ms)	Bumping time (ms)
50 mV				
VD	70	24	0.19	0.04
VU	72	32	0.16	0.08
SD	78	32	0.06	0.18
SU	68	26	0.13	0.05
100 mV				
VD	69	25	0.12	0.05
VU	81	29	0.19	0.06
SD	87	–	0.21	–
SU	69	24	0.09	0.16
150 mV				
VD	67	23	0.08	0.07
VU	81	–	0.30	–
SD	89	–	0.31	–
SU	66	31	0.07	0.18

The errors are estimated to be ±1% for the % blockade current and ±10% for the blockade times.

Table 3. Event frequencies[a] for CY12(+)T1 and CY12(−)T1

Configuration	CY12(+)T1 event frequency (events/min)	CY12(−)T1 event frequency (events/min)
VD	35	500
VU	50	15
SD	150	400
SU	75	15

[a] The frequencies in units of events/min (±10%) were normalized to the equivalent of the addition of 20 µl of 1 mg/ml of peptide.

charge on most proteins is considerably smaller because they tend to have uncharged hydrophobic cores. For example, for RNase A and maltose-binding protein the net charges per residue are +0.032 and −0.021, respectively. Thus, the electrophoretic force will tend to be proportionally smaller and the electroosmotic or other forces may predominate. Indeed, it has recently been shown that the translocation of avidin through silicon nitride pores is driven by electroosmosis at low pHs [41]. As well, because of the reduced net charge density on proteins the effect of voltage on translocation/intercalation times may be small or insignificant. Thus, the question of whether proteins can translocate the α-hemolysin pore may be difficult to answer.

In conclusion, the behavior of simple peptides with the α-hemolysin pore is more complicated than would be expected on the basis of simple electrophoretically driven events. Electroosmotic flow and current rectification due to the pore as well as the dipole moment and charge of the peptide also play significant roles. To distinguish intercalation from simple translocation, it is important to study the effect of voltage on the translocation times.

Acknowledgements

Supported by NSERC with grants to JSL and a graduate scholarship to RIS.

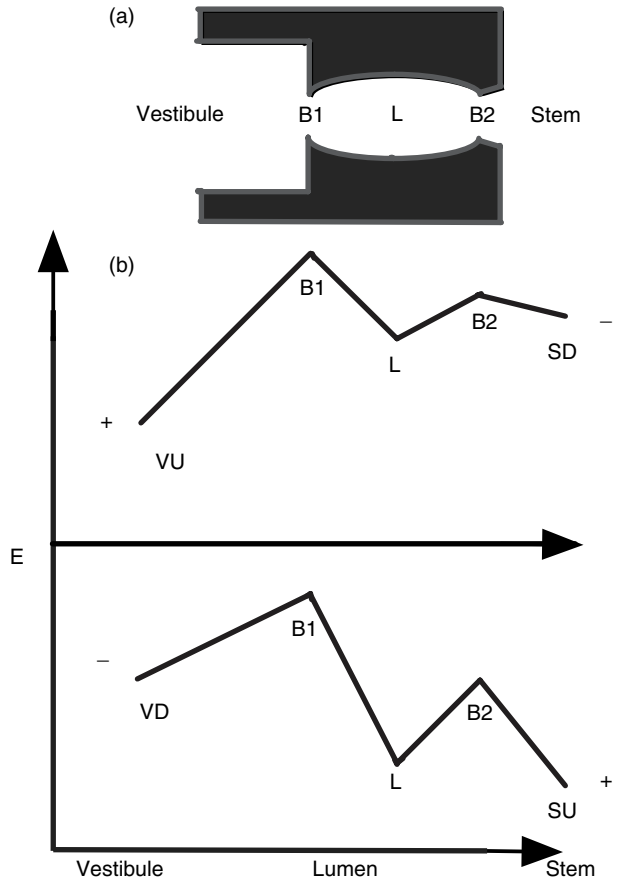

Figure 8. (a) Schematic showing the position of the barriers B1 and B2 relative to the vestibule, lumen and stem. (b) Energy diagrams for CY12(−)T1 in VU and SD configurations (top) and VD and SU configurations (bottom). The electrodes are shown as + and −. The relative heights of B1 and B2 determine the most probable direction of exit from the lumen.

References

1 Song LZ, Hobaugh MR, Shustak C, Cheley S, Bayley H, Gouaux JE. Structure and staphylococcal α-hemolysin, a heptameric transmembrane pore. *Science* 1996; **274**: 1859–1866.
2 Parker MW, Buckley JT, Postma JPM, Tucker AD, Leonard K, Pattus F, Tsernoglou D. Structure of the *Aeromonas* toxin proaerolysin in its water-soluble and membrane-channel states. *Nature* 1994; **367**: 292–295.
3 Dekker C. Solid-state nanpores. *Nat. Nanotechnol.* 2007; **2**: 209–215.
4 Movileanu L. Squeezing a single polypeptide through a nanopore. *Soft Mater.* 2008; **4**: 925–931.
5 Movileanu L. Interrogating single proteins through nanopores: challenges and opportunities. *Trends Biotechnol.* 2009; **27**: 333–341.
6 Bezrukov SM. Ion channels as molecular Coulter counters to probe metabolite transport. *J. Membr. Biol.* 2000; **174**: 1–13.
7 Bayley H, Cremer PS. Stochastic sensors inspired by biology. *Nature* 2001; **413**: 226–230.
8 Martin CR, Siwy ZS. Chemistry, learning nature's way: biosensing with synthetic nanopores. *Science* 2007; **317**: 331–332.
9 Bayley H, Martin CR. Resistive-pulse sensing – from microbes to molecules. *Chem. Rev.* 2000; **100**: 2575–2594.
10 Bayley H. Sequencing single molecules of DNA. *Curr. Opin. Chem. Biol.* 2006; **10**: 628–637.
11 Rhee M, Burns MA. Nanopore sequencing technology: nanopore preparations. *Trends Biotechnol.* 2007; **26**: 1146–1153.
12 Branton D, Deamer DW, Marziali A, Bayley HB, Benner SA, Butler T, Di Ventra M, Garaj S, Hibbs A, Huang X, Jovanovich SB, Krstic PS, Lindsay S, Ling XS, Mastrangelo CH, Meller A, Oliver JS, Pershin YV, Ramsey JM, Riehn R, Soni GV, Tabard-Cossa V, Wanunu M, Wiggin M,

Schloss JA. The potential and challenges of nanopore sequencing. *Nat. Biotechnol.* 2008; **26**: 1146–1153.
13 Deamer DW, Akeson M. Nanopores and nucleic acids: prospects for ultrarapid sequencing. *Trends Biotechnol.* 2000; **18**: 147–151.
14 Meller A, Nivon A, Brandin E, Golovchenko J, Branton D. Rapid nanopore discrimination between single polynucleotide molecules. *Proc. Natl. Acad. Sci. USA* 2006; **19**: 1079–1084.
15 Kasianowicz JJ, Brandin E, Branton D, Deamer DW. Characterization of individual polynucleotide molecules using a membrane channel. *Proc. Natl. Acad. Sci. USA* 1996; **93**: 13770–13773.
16 Sutherland TC, Long Y, Stefureac R, Bediako-Amoa I, Kraatz H, Lee JS. Structure of peptides investigated by nanopore analysis. *Nano Lett.* 2004; **4**: 1273–1277.
17 Movileanu L, Schmittschmitt JP, Scholtz JM, Bayley H. Interactions of peptides with a protein pore. *Biophys. J.* 2005; **89**: 1030–1045.
18 Goodrich CP, Kirmizialtin C, Huyghes-Despointes BM, Zhu A, Scholtz JM, Makarov DE, Movileanu L. Single-molecule electrophoresis of β-hairpin peptides by electrical recordings and langevin dynamics simulations. *J. Phys. Chem. B* 2007; **111**: 3332–3335.
19 Stefureac R, Long Y, Kraatz HB, Howard P, Lee JS. Transport of α-helical peptides through α-hemolysin and aerolysin pores. *Biochem.* 2006; **45**: 9172–9179.
20 Wolfe AJ, Mohammad MM, Cheley S, Bayley H, Movileanu L. Catalyzing the translocation of polypeptides through attractive interactions. *J. Am. Chem. Soc.* 2007; **129**: 14034–14041.
21 Zhao Q, Jayawardhana DA, Wang D, Guan X. Study of peptide transport through engineered protein channels. *J. Phys. Chem. B* 2009; **113**: 3572–3578.
22 Stefureac RI, Lee JS. Nanopore analysis of the folding of zinc fingers. *Small* 2008; **4**: 1646–1650.
23 Stefureac RI, Waldner L, Howard P, Lee JS. Nanopore analysis of a small 86-residue protein. *Small* 2008; **4**: 59–63.
24 Mohammad PS, Matouschek A, Movileanu L. Controlling a single protein in a nanopore through electrostatic traps. *J. Am. Chem. Soc.* 2008; **130**: 4081–4088.
25 Zhao Q, Jayawardhana DA, Wang D, Guan X. Study of peptide transport through engineered protein channels. *J. Phys. Chem.* 2009; **113**: 3572–3578.
26 Bikwemu R, Wolfe AJ, Xing X, Movileanu L. Facilitated translocation of polypeptides through a single nanopore. *J. Phys.* 2010; **22**: 454177–454188.
27 Oukhaled G, Mathe J, Biance AL, Bacri L, Betton JM, Lairez D, Pelta J, Auvray L. Unfolding of proteins and long transient conformations detected by single nanopore recording. *PRL* 2007; **98**: 158101–158104.
28 Madampage CA, Andrievskaia O, Lee JS. Nanopore detection of antibody prion interactions. *Anal. Biochem.* 2010; **396**: 36–41.
29 Stefureac R, Madampage CA, Andrievskaia O, Lee JS. Nanopore analysis of metal ion interactions with prion proteins and peptides. *Biochem. Cell Biol.* 2010; **88**: 1–13.
30 Baran C, Smith GST, Bamm VV, Harauz G, Lee JS. Divalent cations produce a compaction of intrinsically disordered myelin basic protein. *Biochem. Biophys. Res. Comm.* 2010; **391**: 224–229.
31 Apetrei A, Asandei AI, Park Y, Hahm K, Winterhalter M, Luchian T. Unimolecular study of the interaction between the outer membrane protein OmpF from *E. coli* and an analogue of the HP(2–20) antimicrobial peptide.. *J. Bioenerg. Biomembr.* 2010; **42**: 173–180.
32 Patoriza-Gallego M, Rabah L, Gibrat G, Thiebot B, Gisou van der Goot F, Auvray L, Betton J, Pelta J. Dynamics of unfolded protein transport through an aerolysin pore. *J. Am. Chem. Soc.* 2011; **133**: 2923–2931.
33 Oukhaled A, Cressiot B, Bacri L, Patoriza-Gallego M, Betton J, Bourhis E, Jede R, Gierak J, Auvray L, Pelta J. Dynamics of completely unfolded and native proteins through solid-state nanopores as a function of electric driving force. *Nano ACS* 2011; **5**: 3628–3638.
34 Stefureac RI, Trivedi D, Marziali A, Lee JS. Evidence that small proteins translocate through silicon nitride pores in a folded conformation. *J. Phys.* 2010; **22**: 454133–454143.
35 Gu L-Q, Cheley S, Bayley H. Electroosmotic enhancement of the binding of a neutral molecule to a transmembrane pore. *Proc. Natl. Acad. Sci.* 2003; **100**: 15498–15503.
36 Meng H, Detillieux D, Baran C, Krasniqui B, Christensen C, Madampage C, Stefureac RI, Lee JS. Nanopore analysis of tethered peptides. *J. Pept. Sci.* 2010; **16**: 701–708.
37 Mohammad MM, Movileanu L. Excursion of a single polypeptide into a protein pore: simple physics, but complicated biology. *Eur. Biophys. J.* 2008; **27**: 913–925.
38 Timmenman P, Beld J, Puijk WC, Meloen RH. Rapid and quantitative cyclization of multiple peptide loops onto synthetic scaffolds for structural mimicry of protein surfaces. *ChemBioChem.* 2005; **6**: 821–824.
39 Colquhoun D, Sigworth FJ. Fitting and statistical analysis of single-channel records. In *Single-channel Recording*. 2nd edn, Sakmann B, Neher E (eds). Plenum press: New York, 1995; 483–585.
40 Pedone D, Firnkes M, Rant U. Data analysis of translocation events in nanopore experiments. *Anal. Chem.* 2009; **81**: 9689–9694.
41 Firnkes M, Pedone D, Knezevic J, Doblinger M, Rant U. Electrically facilitated translocations of proteins through silicon nitride nanopores: conjoint and competitive action of diffusion, electrophoresis, and electroosmosis. *Nano Lett.* 2010; **10**: 2162–2167.

